ACS Catalysis

Research Article

pubs.acs.org/acscatalysis

# The Rise of Calcination Temperature Enhances the Performance of Cu Catalysts: Contributions of Support

Yifeng Zhu,[†,‡] Xiao Kong,[†,‡] Dong-Bo Cao,[†,§] Jinglei Cui,[†,‡] Yulei Zhu,*[,†,§] and Yong-Wang Li[†,§]

[†]State Key Laboratory of Coal Conversion, Institute of Coal Chemistry, Chinese Academy of Sciences, Taiyuan 030001, P. R. China

[‡]University of Chinese Academy of Sciences, Beijing 100039, P. R. China

[§]Synfuels China Company Ltd., Beijing 101407, P. R. China

Supporting Information

**ABSTRACT:** To develop the high-performance supported metal catalyst for industrial processes, it is highly desirable to elucidate and fully utilize the indispensable support part. Herein, the relationship between catalytic performance and the structure of support $ZrO_2$ was elucidated by comprehensive analysis of the progressive calcination experiments, tests over model catalysts, and various characterizations of catalyst structures. We demonstrated that combination of Cu and tetragonal $ZrO_2$ makes a highly active, selective, and especially stable catalyst for the hydrogenation of dimethyl oxalate to ethylene glycol. To obtain stable Cu particles, the catalyst was annealed at high temperatures (e.g., from 450 to 850 °C). The stable large Cu particles were formed, and the number of exposed Cu sites decreased. Fortunately, support $ZrO_2$ was motivated into the tetragonal phase, compensating for and even improving the activity. Thus, the yield of ethylene glycol was greatly improved from ~26 to 99%, and a stable performance was achieved (life span of >600 h). The strategy alleviated the dependence of hydrogenation on highly dispersed metal sites and provided an alternative way to enhance the catalytic stability. This simple way simultaneously improved the efficiency and reduced the level of irreversible deactivation due to sintering, which has great potential for industrial applications. Tetragonal $ZrO_2$ also proved to be effective for a series of carbonyl hydrogenations (e.g., esters, aldehydes, ketones, and acids), indicating a general promotion of these reactions by $ZrO_2$.

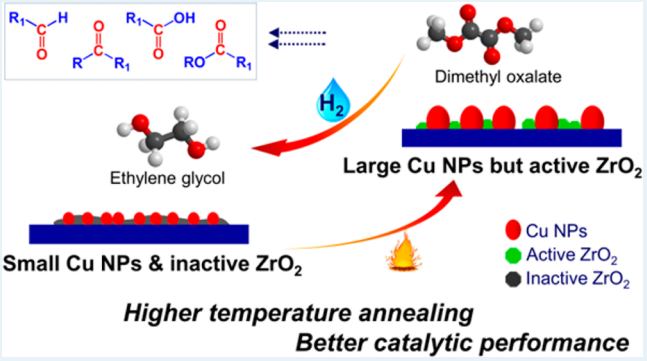


**KEYWORDS:** *catalytic support, cooperative effects, copper, zirconia, stability, catalytic hydrogenation*

## 1. INTRODUCTION

The hydrogenation of C═O and C−O bonds (e.g., $CO/CO_2$, esters, aldehydes, ketones, and acids) is an important facet of synthetic chemistry.[1] Metal nanoparticles (NPs) dispersed on porous supports are always used for these hydrogenation reactions of C═O and C−O bonds. Among the catalysts, Cu catalysts have been intensively explored because they are abundant and inexpensive.[1a] However, there are two limitations of the Cu catalysts, including their inherent activity being lower than that of noble metals and irreversible deactivation mainly due to metal sintering.[1b,2] As Cu sites account for these hydrogenation reactions, the particle size, morphology, defects, and electronic state of Cu often vary depending on the activity.[3] Along this line, dispersing Cu NPs into a few nanometers and modulating their properties are common ways to improve the activity while the filled d orbital of Cu inherently limits the performance to some extent.[2a] The sintering that resulted from the growth of metal particles is mainly due to the low Hüttig (134 °C, the temperature at which defective atoms will diffuse) and Tamman (405 °C, that at which atoms in the bulk will be mobile) temperatures.[2b,4] Some valuable strategies comprise alloying, enhancing metal−support interactions by using specific oxides, and encapsulation of NPs.[1a,c,2b,5] In this study, we demonstrate another option to promote both reactivity and stability.

Generally, dispersing Cu NPs into smaller crystallites can access more metal sites and modulate properties and therefore yield higher activity. However, because the reaction temperatures are always higher than the Hüttig temperature, these small crystallites migrate more easily and possess low stability. On the other hand, annealing Cu NPs into large particles can prolong their lifespans but would cause low activity. To realize the full performance, maximizing the utilization of support is crucial because it is an indispensable part of catalysts. Some supports (e.g., $ZrO_2$, ZnO, $CeO_2$, and $TiO_2$) were reported to participate in hydrogenation of C═O and C−O bonds,[6] while rare reports focused on fully utilizing their potential to improve

Received: May 21, 2014
Revised: September 9, 2014
Published: September 9, 2014

   dx.doi.org/10.1021/cs501155x | ACS Catal. 2014, 4, 3675−3681

both activity and stability, and elucidating their direct contributions.

Inspired by the seemingly irreconcilable conflict between the activity and stability of Cu NPs, we have explored the synergy of tetragonal $ZrO_2$ and Cu and then utilized it to design an efficient and stable catalyst that would efficiently catalyze the hydrogenation of carbonyl compounds. We employed the Cu/$SiO_2$/$ZrO_2$ catalyst to catalyze the hydrogenation of dimethyl oxalate (DMO) to ethylene glycol (EG) (Scheme 1a; see Scheme S1 of the Supporting Information for details) as a showcase. DMO is the simplest diester and a good model compound for studying the selective hydrogenation of C=O and C−O bonds. Moreover, the hydrogenated product EG is a platform chemical for the polymer industry and automotive antifreeze, being consumed at a rate of 20 million tons/year.[7] This reaction is a key element for the syngas-to-EG process, which is important in substituting for the traditional petroleum-based route and achieving cleaner resource utilization.[8] Cu-based catalysts are widely employed for this reaction, while the most severe impediments hindering commercial application are the low catalytic efficiency and the irreversible deactivation.

**Scheme 1. (a) Hydrogenation of DMO (MG, methyl glycolate; EG, ethylene glycol) and (b) Design of a High-Performance Catalyst Using High-Temperature Calcination To Motivate $ZrO_2$ Support and Stabilize Cu Particles**

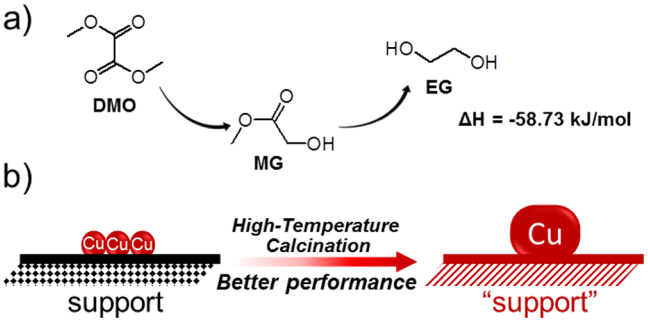


Herein, we report the highly active, selective, and especially stable catalysts for DMO hydrogenation can be obtained by high-temperature calcination (Scheme 1b). The key to our strategy is to motivate amorphous $ZrO_2$ into the active tetragonal phase and anneal Cu NPs into large stable particles by increasing the calcination temperature (CT). $ZrO_2$ can transform from the amorphous (am) phase to the tetragonal (t) phase and then to the monoclinic (m) phase at elevated CTs, at which the crystal phases exhibited better catalytic performance.[9] The high-temperature calcination (e.g., 850 °C) induced the large Cu NPs and caused the loss of active Cu sites. It also integrated the stable large Cu NPs with active $ZrO_2$ and facilitated the efficient and stable EG synthesis from DMO hydrogenation. Besides, it eliminated the surface acid sites, suppressing byproduct formation.[4b,10] Thus, the catalyst produced a greatly improved EG yield of 99% and stability (life span of >600 h), which is the highest that has been reported to the best of our knowledge. These results alleviate the dependence of highly dispersed metal sites and provide a new option for designing a high-performance catalyst for industrial DMO hydrogenation. We proved the role of t-$ZrO_2$ and also applied this knowledge to a range of carbonyl hydrogenations (esters, aldehydes, ketones, and acids). t-$ZrO_2$ could significantly promote the hydrogenation of these carbonyl compounds. Thus, a general promotion effect of t-$ZrO_2$ on the hydrogenation of carbonyls emerged and was expected to have great implications for further mechanistic studies.

## 2. EXPERIMENTAL SECTION

**2.1. Catalyst Preparation.** The samples were prepared by coprecipitation with a $NH_4HCO_3$ solution as a precipitator. The copper nitrate and/or support precursors (zirconium nitrate and/or acidic silica sol) were mixed and dissolved in water. Then, the solution was introduced into a 2 L precipitation vessel at 70 °C. At the same time, an aqueous solution of $NH_4HCO_3$ was dripped into this vessel to maintain the pH at 5 ± 0.2. The precipitates were aged, filtered, washed, dried, and then calcined in air.[4b] Cu/$SiO_2$, Cu/$ZrO_2$, and Cu/$SiO_2$/$ZrO_2$ catalysts are denoted as CuSi-*T*, CuZr-*T*, and CuSiZr*x*-*T*, respectively, where *T* is CT and *x* is the $SiO_2$/$ZrO_2$ mass ratio. CuO and $ZrO_2$ were prepared by procedures similar to those used to prepare the catalysts. The CuO+$ZrO_2$ model catalyst was prepared by physically mixing CuO and $ZrO_2$ samples.

**2.2. Evaluation.** Evaluations were conducted on a fixed-bed reactor. Prior to the tests, the catalysts (20−40 mesh) were activated by in situ reduction at 250 °C in a dilute $H_2$ flow. The products were condensed in a cold trap and then analyzed using a gas chromatography instrument (DB-WAXETR column) equipped with a flame ionization detector.

**2.3. Catalyst Characterization.** The composition of catalysts was determined by ICP-OES (Optima2100DV, PerkinElmer). BET surface areas were characterized by $N_2$

**Table 1. Performance of Cu/$SiO_2$, Cu/$ZrO_2$, and Cu/$SiO_2$/$ZrO_2$ Catalysts with Different $SiO_2$/$ZrO_2$ Ratios[a]**

| catalyst | Cu (wt %)[b] | $SiO_2$/$ZrO_2$ ratio (g/g)[b] | $S_{BET}$ ($m^2$/g)[c] | $D_{Cu}$ (%)[d] | $S_{Cu}$ ($m^2$/g)[d] | TOF[1] ($h^{-1}$) | TOF[2] ($h^{-1}$) | conversion (%) | selectivity (%)[e] | | | |
|---|---|---|---|---|---|---|---|---|---|---|---|---|
| | | | | | | | | | EG | MG | ethanol | others |
| CuSi-650 | 39.8 | ∞ | 93.9 | 1.4 | 3.6 | 3.3 | 3.3 | 11.8 | 0.9 | 97.5 | 1.6 | 0 |
| CuSiZr9-650 | 39.6 | 8.1 | 78.7 | 2.4 | 6.6 | 11.3 | 11.1 | 73.0 | 15.5 | 82.8 | 0.4 | 1.3 |
| CuSiZr2-650 | 37.9 | 1.8 | 77.4 | 5.9 | 15.1 | 11.3 | 10.6 | 98.6 | 55.5 | 43.0 | 0.5 | 1.0 |
| CuSiZr1-650 | 37.0 | 0.9 | 73.4 | 6.1 | 15.3 | 13.2 | 11.8 | 100 | 98.5 | 0.5 | 0.5 | 0.5 |
| CuSiZr0.5-650 | 36.4 | 0.5 | 56.5 | 3.2 | 8.0 | 14.9 | 13.8 | 98.3 | 67.5 | 31.4 | 0.3 | 0.8 |
| CuZr-650 | 34.8 | 0 | 30.0 | 3.1 | 7.2 | 15.0 | 14.2 | 98.1 | 66.1 | 32.8 | 0.4 | 0.7 |

[a]At 190 °C, 3 MPa, 0.3 $h^{-1}$, and 150 mol of $H_2$/mol of DMO. TOFs were calculated at EG yields of less than ∼10% and DMO conversions of less than ∼50% to obtain the intrinsic activities. TOF[1] was calculated on the basis of the converted ester group and TOF[2] on the basis of the converted DMO (see the Supporting Information for details). [b]Determined by ICP-OES. [c]Determined by $N_2$ physical adsorption. [d]Determined by $N_2O$ titration. [e]Others mainly comprise 2-methoxyethanol, 1,2-propanediol, and 1,2-butanediol.


dx.doi.org/10.1021/cs501155x | ACS Catal. 2014, 4, 3675−3681

physical adsorption at −196 °C (Micromeritics ASAP 2420 instrument). $N_2O$ titration (Auto Chem. II 2920, Micromeritics) was employed to determine the Cu dispersions and specific Cu surface areas. The $NH_3$-TPD experiments were performed on the Auto Chem. II 2920 instrument with a mass spectrometer as the detector. Powder X-ray diffraction (XRD) patterns were measured with a X-ray diffractometer (D8 Advance). Raman spectra was measured with a LabRAM HR800 system. The X-ray photoelectron spectroscopy experiments were performed on a VG MiltiLab 2000 spectrometer. High-resolution transmission electron microscopy (HRTEM) was conducted with a JEM-2100F high-resolution instrument at 200 keV. The structural parameters of t-$ZrO_2$ were obtained by Rietveld refinement via XRD. For more details, see the Supporting Information.

## 3. RESULTS AND DISCUSSION

**3.1. Influence of $SiO_2/ZrO_2$ Ratios.** The synthesis of EG from DMO hydrogenation involves stepwise hydrogenation of ester groups (from DMO to MG, and then to EG), as illustrated in Scheme 1a. For this study, we prepared the catalysts by industrial precipitation and optimized the composition by varying the $SiO_2/ZrO_2$ ratio (Table 1). The CuSiZr1-650 catalyst with a nominal $SiO_2/ZrO_2$ ratio of 1 (grams per gram) exhibited the best activity among the catalysts. An important reason is the large accessible Cu sites as a result of the combined effect of the physical dispersion ability and strong metal−support interaction, which has been proven to be a general facet of hydrogenation reactions.[3b,9c] The dense $ZrO_2$ resulted in the loss of BET surface area. It also yielded the enhanced strong metal−support interactions, as evidenced by the red shifts and broadening of Raman peaks (Figure 1). The

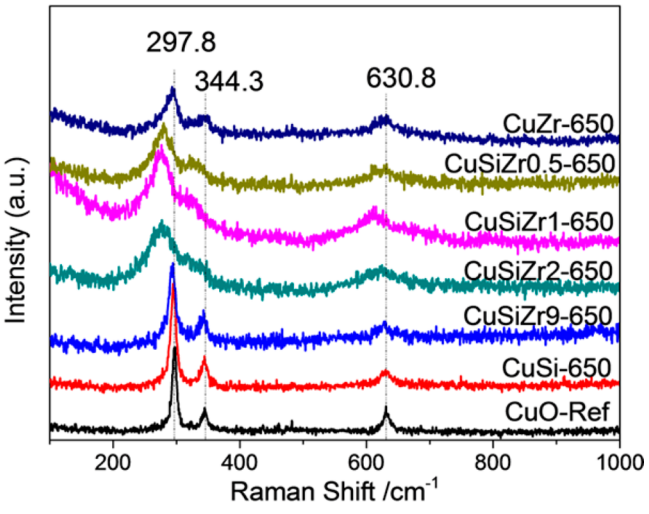


**Figure 1.** Raman spectra of calcined catalysts with different $SiO_2/ZrO_2$ ratios and the reference CuO (CuO-Ref).

bands at 297.8, 344.3, and 630.8 $cm^{-1}$ can be attributed to the vibrations of Cu−O bonds in the CuO lattice.[11] According to our previous work, the red shifts and broadening of peaks indicated strong interactions between Cu and $ZrO_2$ and the incorporation of $Cu^{2+}$ into the supports.[4b]

However, $ZrO_2$-containing catalysts have intrinsic activities significantly higher than that of the CuSi catalyst, which were evaluated by turnover frequencies (TOFs, determined by dividing the activity by the Cu surface area). Herein, we present two kinds of TOFs, which were based on the converted ester groups per site per time ($TOF^1$) and the converted DMO per site per time ($TOF^2$). The Cu LMM X-ray-excited Auger spectroscopy (XAES) spectra of reduced catalysts all exhibited the evident peak at ∼918.8 eV ($Cu^0$) and a negligible peak at ∼916.5 eV ($Cu^+$), indicating that the Cu species over the catalyst surface existed mainly in a metallic state (Figure S1 of the Supporting Information).[3c,12] The site for TOF calculation was thus based on the metallic Cu surface sites. The intrinsic activities could not be simply explained by the Cu state and indicated that $ZrO_2$ may participate during DMO hydrogenation.

**3.2. Roles of $ZrO_2$ in Dimethyl Oxalate Hydrogenation.** To verify that $ZrO_2$ does not work only as a disperser, we thus investigated Cu/$SiO_2$ (CuSi), Cu/$ZrO_2$ (CuZr), and Cu/$SiO_2$/$ZrO_2$ (CuSiZr1) catalysts annealed at progressively elevated temperatures (Table 2). The numbers attached to the notations are relative CTs in degrees Celsius. The CuSiZr1 catalyst calcined at a higher temperature had a smaller Cu specific area but surprisingly exhibited much better performance. A similar trend was also observed over CuZr catalysts. The CuSiZr1 catalysts calcined in the range of 450−650 °C exhibited similar DMO conversion but had dramatically different distributions of MG and EG. Considering the stepwise nature of the reaction process, the different product distributions could be attributed to the different catalytic ability of catalysts in hydrogenation of ester groups. The higher EG yield and lower MG yield indicated better catalytic abilities. TOFs (both $TOF^1$ and $TOF^2$) over CuSiZr1-850 were >7-fold greater than those over CuSiZr1-450. The best EG yields were obtained over CuSiZr1 calcined at 650−850 °C. Excessive surface acid sites would catalyze side reactions, including C−O hydrogenolysis, C−OH etherification, and C−C coupling.[4b,10] The high CT also significantly reduced the number of surface acid sites of CuSiZr1 catalysts (Figure S2 of the Supporting Information) and suppressed byproduct formation (Table 2). From the results described above, a CT of >650 °C emerged as a key parameter in yielding higher activity. If the active sites arise from Cu species only, the EG yield would decrease with no evident change in TOFs at higher CTs, because of the loss of Cu sites. The enhanced activities and TOFs strikingly indicated that the catalytic efficiency is greatly influenced by $ZrO_2$, not merely determined by Cu sites. CuSi-450 showed an unsatisfied activity, while CuSi-650 exhibited a much lower efficiency, implying that $SiO_2$ mainly acted as a physical spacer to disperse other components and was not related to the improvement. It should be noted that although $SiO_2$ functions as a physical spacer, it is an important part of the good performance, considering that the CuSiZr1 catalysts gave EG yields better than those of CuZr catalysts.

To find a structural explanation, XRD experiments with CuSiZr1 and $ZrO_2$ calcined at elevated temperatures were performed (Figure 2). For $ZrO_2$, t-$ZrO_2$ crystallized from the am state after being calcined at 350 °C, as evidenced by the peak at 30.3° (PDF 50-1089). The structure was not stable above 400 °C. When the temperature was further increased, m-$ZrO_2$ (PDF 37-1484) appeared and the peaks intensified with the disappearance of t-$ZrO_2$. However, for CuSiZr1, t-$ZrO_2$ appeared distinctly when the CT was increased to 650 °C, as well as CuZr (Figure S3 of the Supporting Information). t-$ZrO_2$ was stabilized, and the transformation of t-$ZrO_2$ to m-$ZrO_2$ was greatly retarded because of the vacancies introduced by the incorporation of few $Cu^{2+}$ ions.[13] The phase transformation


dx.doi.org/10.1021/cs501155x | ACS Catal. 2014, 4, 3675−3681

**Table 2. Performance of Catalysts Calcined at Elevated CTs and Concept Catalysts[a]**

| | | | | | | | selectivity (%)[d] | | | |
|---|---|---|---|---|---|---|---|---|---|---|
| catalyst | $S_{BET}$ ($m^2/g$)[b] | $D_{Cu}$ (%)[c] | $S_{Cu}$ ($m^2/g$)[c] | TOF[1] ($h^{-1}$) | TOF[2] ($h^{-1}$) | conversion (%) | EG | MG | ethanol | others |
| CuSi-450 | 95.3 | 2.0 | 5.0 | 2.6 | 2.5 | 12.1 | 8.2 | 86.1 | 3.3 | 2.4 |
| CuSi-650 | 93.9 | 1.4 | 3.6 | 3.3 | 3.3 | 11.8 | 0.9 | 97.5 | 1.6 | 0 |
| CuZr-450 | 45.8 | 10.9 | 22.8 | 2.3 | 2.2 | 48.9 | 8.0 | 79.5 | 1.3 | 11.2 |
| CuZr-650 | 30.0 | 3.1 | 7.2 | 15.0 | 14.2 | 98.1 | 66.1 | 32.8 | 0.4 | 0.7 |
| CuSiZr1-450 | 88.3 | 13.7 | 34.2 | 4.3 | 4.2 | 96.5 | 27.1 | 66.4 | 0.4 | 6.1 |
| CuSiZr1-550 | 81.9 | 10.5 | 26.2 | 5.7 | 5.4 | 100 | 89.2 | 7.1 | 0.6 | 3.1 |
| CuSiZr1-650 | 73.4 | 6.1 | 15.3 | 13.2 | 11.8 | 100 | 98.5 | 0.5 | 0.5 | 0.5 |
| CuSiZr1-750 | 65.6 | 3.0 | 7.6 | 28.0 | 24.4 | 100 | 98.2 | 0.5 | 0.4 | 0.9 |
| CuSiZr1-850 | 48.4 | 2.6 | 6.4 | 34.6 | 30.0 | 100 | 99.0 | 0.3 | 0.4 | 0.3 |
| CuO-ref | – | 0.3 | 2.0 | 5.6 | 5.5 | 10.5 | 1.3 | 98.7 | 0 | 0 |
| $ZrO_2$ | – | – | – | – | – | 0 | – | – | – | – |
| CuO+$ZrO_2$ | – | – | – | 20.2 | 19.4 | 26.9 | 6.3 | 92.0 | 0.8 | 0.9 |

[a]At 190 °C, 3 MPa, 0.3 $h^{-1}$, and 150 mol of $H_2$/mol of DMO. TOFs were calculated at EG yields of less than ~10% and DMO conversions of less than ~50% to obtain the intrinsic activities. TOF[1] was calculated on the basis of the converted ester group and TOF[2] on the basis of the converted DMO (see the Supporting Information for details). [b]Determined by $N_2$ physical adsorption. [c]Determined by $N_2O$ titration. [d]Others mainly comprise 2-methoxyethanol, 1,2-propanediol, and 1,2-butanediol.

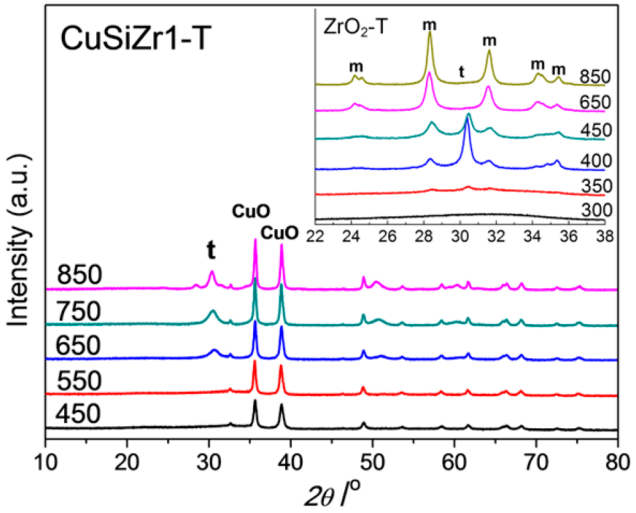


**Figure 2.** XRD patterns of CuSiZr1-*T* and $ZrO_2$-*T* (where *T* above the line means relative CT; t, t-$ZrO_2$; m, m-$ZrO_2$).

seems to be coincident with the change in activity, indicating that the improvement may arise from the participation of t-$ZrO_2$.

Hence, model catalysts were designed (Table 2). The CuO reference (CuO-ref) exhibited a low DMO conversion and EG yield, while $ZrO_2$ (calcined at 400 °C, t phase percentage of 95%[14]) has no activity under the conditions. Interestingly, the EG yield and TOF were greatly increased when CuO was physically mixed with t-$ZrO_2$. The rational explanation is that Cu−t-$ZrO_2$ synergy promoted the reaction, not merely Cu or t-$ZrO_2$. The intermediate MG was also converted in separate experiments over CuO and CuO+t-$ZrO_2$ catalysts to explore the catalytic roles of the $ZrO_2$ component. The CuO+t-$ZrO_2$ mixture showed an MG conversion and an EG yield greater than those of pure CuO, implying that $ZrO_2$ promoted the hydrogenation processes of ester groups. Thus, we concluded that DMO was reduced to EG via two parallel routes, one catalyzed by Cu NPs and the other catalyzed by the synergy sites between Cu and $ZrO_2$ (Scheme S2 of the Supporting Information). The latter route can alleviate the dependence on highly dispersed metal sites for hydrogenation and provide an alternative way to the enhancement of catalyst stability (see below).[15] Similar phenomena were also observed in DMO and MG hydrogenation over CuO+m-$ZrO_2$ (Tables S2 and S3 of the Supporting Information), which are beyond the scope of this study and will be addressed in a forthcoming study.

The unique role of t-$ZrO_2$ was further confirmed by correlating its structural parameters with the catalytic performance (Figure 3). The t phase originates from the cubic fluorite

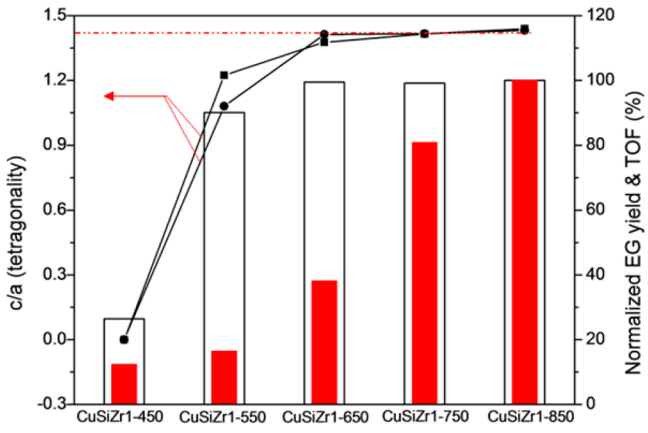


**Figure 3.** c/a and catalytic activities of CuSiZr1-*T* catalysts (circles and squares refer to c/a of reduced and unreduced samples, respectively; the dashed line is ideal c/a; the outer and inner bars are the normalized EG yields and TOFs, respectively; the highest normalized value is 100%). Reaction conditions: 190 °C, 3 MPa, 0.3 $h^{-1}$, and 150 mol of $H_2$/mol of DMO.

phase by the motion of oxygen along one axis, of which ideal c/a (tetragonality) is ~1.4317.[16] The c/a of CuSiZr1-450 was denoted zero because no t phase was observed over the sample. With the increase in CT, the c/a of CuSiZr1 samples showed a tendency toward the ideal value. The results indicated that t-$ZrO_2$ was formed and stabilized upon calcination. In the histogram in Figure 3, the normalized EG yield increased first and then remained at a certain level (~100%); the TOFs calculated on the basis of Cu sites continuously increased. The correlations rationalized the contribution of t-$ZrO_2$ on the hydrogenation of DMO to EG.


dx.doi.org/10.1021/cs501155x | ACS Catal. 2014, 4, 3675−3681

We have proven that t-$ZrO_2$ contributes to the reaction and demonstrated that combination of Cu and t-$ZrO_2$ makes an active catalyst. Both the activity and selectivity are closely related to the real active sites created by Cu and $ZrO_2$. $ZrO_2$ is able to enhance the activity during $CO_2$ hydrogenation.[17] It was found that the adsorption energies of $CO_2$ and O-containing intermediates (e.g., OH, HCO, $H_2CO$, HCOO, $H_2COO$, $H_3CO$, and $H_2COOH$) on the Cu(111)/m-$ZrO_2$(−111) interface are much higher than those of Cu(111), using density functional theory methods. The adsorption of these species on $ZrO_2$ was also confirmed by infrared spectra.[17a,b,d] Considering the much lower barrier for $H_2$ dissociative adsorption on Cu sites compared to that on $ZrO_2$, $CO_2$ hydrogenation is favored to occur at the Cu/$ZrO_2$ interface. Thus, it is believed that $ZrO_2$ promotes the adsorption and activation of carbonyls and facilitates the reactions of O-containing intermediates.[15] How the carbonyl groups and H atoms reacted over Cu/$ZrO_2$ sites remains elusive and will be addressed in our future work.

HRTEM images of reduced CuZr-650 and CuSiZr1-650 are shown in Figure 4. The *d* spacings of ∼0.209 and ∼0.297 nm

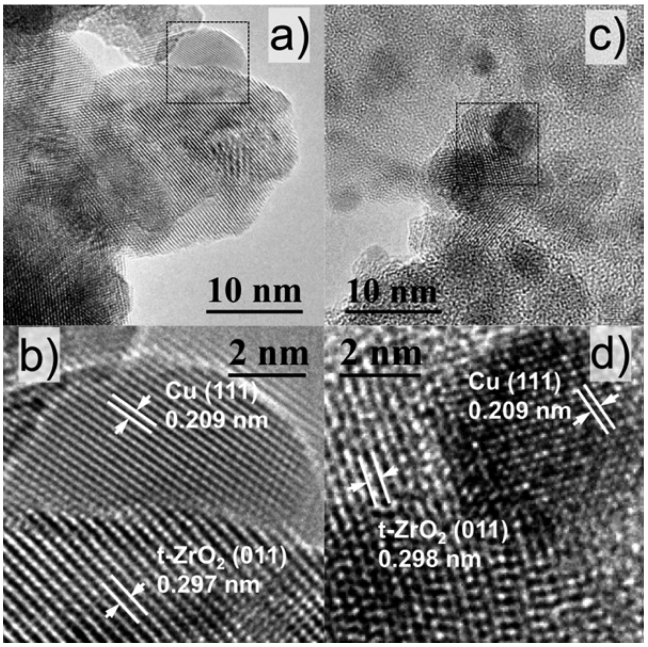


**Figure 4.** HRTEM images of reduced CuZr-650 (a and b) and CuSiZr1-650 (c and d).

correspond to the Cu(111) and t-$ZrO_2$(011) plane, respectively. The selected area electron diffraction patterns of catalysts confirmed the presence of these planes (Figure S4 of the Supporting Information). In line with XRD results (Figure S5 of the Supporting Information), larger Cu and t-$ZrO_2$ NPs were observed over CuZr than over CuSiZr1. Cu and t-$ZrO_2$ domains were intimately contacted, which generated a large interface. With respect to the synergy effect and minimized transport distance, the interfaces should be more active where both Cu and $ZrO_2$ contribute to the reaction.[18] In addition, roles of defects and/or vacancies cannot be ruled out. These sites can be produced by doping of $Cu^{2+}$ into t-$ZrO_2$, $Cu^{2+}$ reduction, and departure of oxygen from t-$ZrO_2$. A slight shift toward a lower binding energy appeared over Zr 3d spectra of reduced samples with increasing CTs, while no change was observed over the unreduced samples (Figure S6 of the Supporting Information). It can be attributed to the formation of Zr species with relatively higher electron density.[9c] These species upon reduction have coordination numbers lower than those of the bulk and may be associated with the oxygen vacancies over the interfaces, which can stabilize intermediates and lower the activation barriers.[19] Oxygen extraction would also introduce Cu atoms into t-$ZrO_2$ and result in some changes on the Cu side. However, a negligible difference was observed because large Cu NPs exhibit mainly the bulk properties and conceal the information about defects and/or interfacial sites.[3b]

The most severe problem inherent to Cu catalysts is the irreversible deactivation by sintering. The high CT would not only facilitate the formation of t-$ZrO_2$ and provide the unique route catalyzed by Cu/t-$ZrO_2$ synergy but also induce larger and more stable Cu particles. In this sense, the catalysts annealed at high temperatures may not only reserve the high activity but also exhibit steady performance. CuSiZr1-850 was very stable for >600 h with an EG yield of >96%, which is better than those of any catalysts ever reported and convinced us of our assumption (Figure 5). To the best of our knowledge,

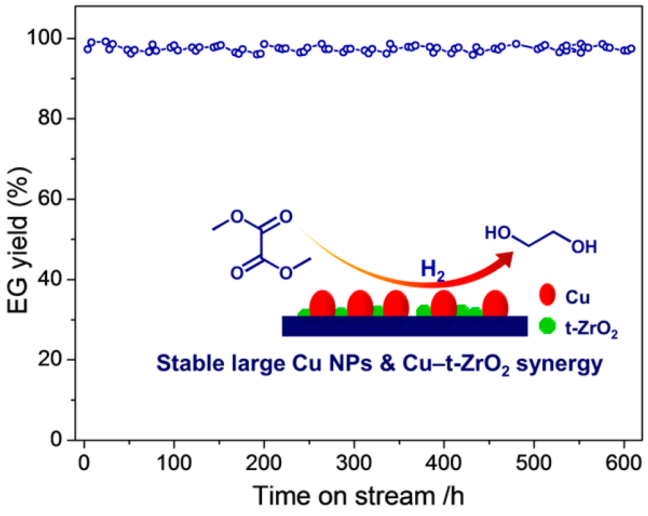


**Figure 5.** Stability of the CuSiZr1-850 catalyst. Reaction conditions: 190 °C, 3 MPa, 0.3 $h^{-1}$, and 150 mol of $H_2$/mol of DMO.

this is the first report of such exceptional improvement in both stability and efficiency for DMO hydrogenation by annealing the Cu NPs into large and stable particles and utilizing the active $ZrO_2$. Thus, this method via a unique but simple way (high-temperature calcination on Cu/$ZrO_2$ phases) alleviates the need to use precious metal (e.g., Au[20]) to promote activity and simultaneously obtain large and inherently stable metal NPs that are difficult to deactivate. Besides, the high CT would make the catalysts denser and increase the EG capacity, because a giving reactor can load more catalysts. These desired features give the catalyst great potential for industrial applications.

**3.3. Applications for the Reduction of Carbonyl Compounds.** The reduction of carbonyl groups (e.g., esters, aldehydes, ketones, and acids) is one of the most fundamental and widely employed reactions.[21] The role of t-$ZrO_2$ was then extended to this kind of reaction. We used the hydrogenation of methyl acetate, *n*-propanal, acetone, and acetic acid over concept catalysts as models (Table 3). CuO-ref showed low activities for these reactions, while the efficiencies were greatly improved when CuO-ref was mixed with $ZrO_2$ (calcined at 400


dx.doi.org/10.1021/cs501155x | ACS Catal. 2014, 4, 3675−3681

**Table 3. Hydrogenation of Carbonyl Compounds over Concept Catalysts[a]**

| entry | catalyst | $T$ (°C) | conversion (%) | selectivity (%) |
|---|---|---|---|---|
| methyl acetate | CuO-ref | 250 | 7.7 | 100[b] |
| | $CuO+ZrO_2$ | 250 | 37.0 | 100[b] |
| *n*-propanal | CuO-ref | 260 | 8.4 | 100[c] |
| | $CuO+ZrO_2$ | 260 | 69.1 | 97.0[c] |
| acetone | CuO-ref | 220 | 8.6 | 100[d] |
| | $CuO+ZrO_2$ | 220 | 96.6 | 98.2[d] |
| acetic acid | CuO-ref | 290 | 3.6 | 93.5[e] |
| | $CuO+ZrO_2$ | 290 | 51.3 | 91.5[e] |

[a]At 4 MPa, 0.3 $h^{-1}$, and 100 mol of $H_2$/mol of substrate. [b]Ethanol. [c]*n*-Propanol. [d]Isopropanol. [e]Acetaldehyde and ethanol.

°C). The results here indicated that the roles of $ZrO_2$ upon hydrogenation of DMO could be generalized into hydrogenation of esters, aldehydes, ketones, and acids, facilitating future work on the $Cu/ZrO_2$ synergy for hydrogenation reactions. Moreover, considering the roles of the $ZrO_2$ support, our work to improve both activity and stability may also be effective for the hydrogenation of carbonyl groups.

## 4. CONCLUSIONS

In summary, we demonstrated the direct contribution of support $ZrO_2$ to the hydrogenation of DMO and a series of carbonyl compounds. The relationship between catalytic performance and the structure of support $ZrO_2$ was elucidated by using the progressive calcination experiments, tests over model catalysts, and various characterizations of catalyst structures. Moreover, we showed how the structure−performance relationship and the contributions of $ZrO_2$ can facilitate the design of a high-performance catalyst. To obtain a highly stable catalyst, we annealed the Cu NPs into large and stable particles at high temperatures. In the meantime, $ZrO_2$ was motivated into an active tetragonal phase, which greatly compensated for and promoted the catalytic efficiency. The high-temperature calcination also eliminated the surface acid sites, facilitating EG production. The resulting $Cu/SiO_2/ZrO_2$ catalysts prepared by a simple coprecipitation method and high-temperature calcination exhibited a high EG yield of ∼99% and high stability (>600 h), rendering them promising materials for industrial hydrogenation of DMO to EG. The promotional roles of $ZrO_2$ can be generalized into hydrogenation of carbonyl compounds, including esters, aldehydes, ketones, and acids. Our study highlights the design of highly active, selective, and stable Cu catalysts via a simple way, simultaneously solving the low reactivity and deactivation caused by sintering for supported metal catalysts. The results will be useful in the development of supported metal catalysts for a range of hydrogenation reactions of carbonyl compounds and have great implications for practical applications.

## ■ ASSOCIATED CONTENT

### Supporting Information

Experimental details, details of the background of the model reaction (Scheme S1), representation of possible routes of DMO hydrogenation over $Cu/ZrO_2$ catalysts (Scheme S2), details of Rietveld refinement (Table S1), MG hydrogenation over model catalysts (Table S2), DMO hydrogenation over model catalysts (Table S3), Cu LMM XAES spectra (Figure S1), $NH_3$-TPD profiles (Figure S2), XRD spectra of catalysts (Figures S3 and S5), SAED patterns of catalysts (Figure S4), and Zr 3d spectra of catalysts (Figure S6). This material is available free of charge via the Internet at http://pubs.acs.org.

## ■ AUTHOR INFORMATION


### Corresponding Author

*E-mail: zhuyulei@sxicc.ac.cn. Telephone: +86 351 7117097. Fax: +86 351 7560668.


### Author Contributions

Y.Z., X.K., and Y.Z. designed and performed the experiments and wrote the paper. D.-B.C., J.C., and Y.-W.L. discussed the role of support and helped write the paper. Y.-W.L. also helped choose the model reactions.

### Notes

The authors declare no competing financial interest.

## ■ ACKNOWLEDGMENTS

We thank Dr. G. Ding for helpful suggestions. This work was supported by the Major State Basic Research Development Program of China (973 Program, 2012CB215305).

## ■ REFERENCES


(1) (a) O'Neill, B. J.; Jackson, D. H.; Crisci, A. J.; Farberow, C. A.; Shi, F.; Alba-Rubio, A. C.; Lu, J.; Dietrich, P. J.; Gu, X.; Marshall, C. L.; Stair, P. C.; Elam, J. W.; Miller, J. T.; Ribeiro, F. H.; Voyles, P. M.; Greeley, J.; Mavrikakis, M.; Scott, S. L.; Kuech, T. F.; Dumesic, J. A. *Angew. Chem., Int. Ed.* **2013**, *52*, 13808−13812. (b) Prieto, G.; Zecevic, J.; Friedrich, H.; de Jong, K. P.; de Jongh, P. E. *Nat. Mater.* **2013**, *12*, 34−39. (c) Yue, H.; Zhao, Y.; Zhao, S.; Wang, B.; Ma, X.; Gong, J. *Nat. Commun.* **2013**, *4*, 2339−2345.

(2) (a) Hagen, J. Heterogeneous Catalysis: Fundamentals. In *Industrial Catalysis: A Practical Approach*, 2nd ed.; VCH: Weinheim, Germany, 1999; pp 99−222. (b) Cao, A.; Lu, R.; Veser, G. *Phys. Chem. Chem. Phys.* **2010**, *12*, 13499−13510.

(3) (a) Kasatkin, I.; Kurr, P.; Kniep, B.; Trunschke, A.; Schlögl, R. *Angew. Chem.* **2007**, *119*, 7465−7468. (b) Behrens, M.; Studt, F.; Kasatkin, I.; Kühl, S.; Hävecker, M.; Abild-Pedersen, F.; Zander, S.; Girgsdies, F.; Kurr, P.; Kniep, B. L.; Tovar, M.; Fischer, R. W.; Nørskov, J. K.; Schlögl, R. *Science* **2012**, *336*, 893−897. (c) Gong, J.; Yue, H.; Zhao, Y.; Zhao, S.; Zhao, L.; Lv, J.; Wang, S.; Ma, X. *J. Am. Chem. Soc.* **2012**, *134*, 13922−13925.

(4) (a) Yue, H.; Zhao, Y.; Zhao, L.; Lv, J.; Wang, S.; Gong, J.; Ma, X. *AIChE J.* **2012**, *58*, 2798−2809. (b) Zhu, Y.; Zhu, Y.; Ding, G.; Zhu, S.; Zheng, H.; Li, Y. *Appl. Catal., A* **2013**, *468*, 296−304.

(5) (a) Farmer, J. A.; Campbell, C. T. *Science* **2010**, *329*, 933−936. (b) Cao, A.; Veser, G. *Nat. Mater.* **2010**, *9*, 75−81. (c) Lu, J.; Fu, B.; Kung, M. C.; Xiao, G.; Elam, J. W.; Kung, H. H.; Stair, P. C. *Science* **2012**, *335*, 1205−1208.

(6) (a) Comotti, M.; Li, W.-C.; Spliethoff, B.; Schüth, F. *J. Am. Chem. Soc.* **2006**, *128*, 917−924. (b) Rodriguez, J. A.; Graciani, J.; Evans, J.; Park, J. B.; Yang, F.; Stacchiola, D.; Senanayake, S. D.; Ma, S.; Perez, M.; Liu, P.; Fdez Sanz, J.; Hrbek, J. *Angew. Chem., Int. Ed.* **2009**, *48*, 8047−8050. (c) Shekhar, M.; Wang, J.; Lee, W. S.; Williams, W. D.; Kim, S. M.; Stach, E. A.; Miller, J. T.; Delgass, W. N.; Ribeiro, F. H. *J. Am. Chem. Soc.* **2012**, *134*, 4700−4708. (d) Zander, S.; Kunkes, E. L.; Schuster, M. E.; Schumann, J.; Weinberg, G.; Teschner, D.; Jacobsen, N.; Schlögl, R.; Behrens, M. *Angew. Chem., Int. Ed.* **2013**, *52*, 6536−6540.

(7) Wang, A.; Zhang, T. *Acc. Chem. Res.* **2013**, *46*, 1377−1386.

(8) (a) Chen, L.; Guo, P.; Qiao, M.; Yan, S.; Li, H.; Shen, W.; Xu, H.; Fan, K. *J. Catal.* **2008**, *257*, 172−180. (b) Zheng, X.; Lin, H.; Zheng, J.; Duan, X.; Yuan, Y. *ACS Catal.* **2013**, *3*, 2738−2749.

(9) (a) Chang, S.-m.; Doong, R.-a. *Chem. Mater.* **2005**, *17*, 4837−4844. (b) Lin, C.; Zhang, C.; Lin, J. *J. Phys. Chem. C* **2007**, *111*, 3300−3307. (c) Wang, L.-C.; Liu, Q.; Chen, M.; Liu, Y.-M.; Cao, Y.; He, H.-Y.; Fan, K.-N. *J. Phys. Chem. C* **2007**, *111*, 16549−16557. (d) Sato, A.

G.; Volanti, D. P.; Meira, D. M.; Damyanova, S.; Longo, E.; Bueno, J. M. C. *J. Catal.* **2013**, *307*, 1−17.
(10) Yue, H.; Ma, X.; Gong, J. *Acc. Chem. Res.* **2014**, *47*, 1483−1492.
(11) Irwin, J.; Wei, T. *J. Phys.: Condens. Matter* **1999**, *3*, 299−306.
(12) Yin, A.; Guo, X.; Dai, W.; Fan, K. *J. Phys. Chem. C* **2009**, *113*, 11003−11013.
(13) (a) Wang, Y.; Caruso, R. A. *J. Mater. Chem.* **2002**, *12*, 1442−1445. (b) Štefanić, G.; Musić, S.; Ivanda, M. *J. Alloys Compd.* **2010**, *491*, 536−544.
(14) Xie, H.; Lu, J.; Shekhar, M.; Elam, J. W.; Delgass, W. N.; Ribeiro, F. H.; Weitz, E.; Poeppelmeier, K. R. *ACS Catal.* **2013**, *3*, 61−73.
(15) Peng, B.; Yuan, X.; Zhao, C.; Lercher, J. A. *J. Am. Chem. Soc.* **2012**, *134*, 9400−9405.
(16) Yashima, M. *J. Phys. Chem. C* **2009**, *113*, 12658−12662.
(17) (a) Fisher, I. A.; Woo, H. C.; Bell, A. T. *Catal. Lett.* **1997**, *44*, 11−17. (b) Kwang-Deog, J.; Alexis, T. B. *J. Catal.* **2000**, *193*, 207−223. (c) Tang, Q.-L.; Hong, Q.-J.; Liu, Z.-P. *J. Catal.* **2009**, *263*, 114−122. (d) Pokrovski, K.; Jung, K. T.; Bell, A. T. *Langmuir* **2001**, *17*, 4297−4303. (e) Jung, K. T.; Bell, A. T. *Catal. Lett.* **2002**, *80*, 63−68.
(18) Arrii, S.; Morfin, F.; Renouprez, A.; Rousset, J. *J. Am. Chem. Soc.* **2004**, *126*, 1199−1205.
(19) (a) Yang, Y.; Evans, J.; Rodriguez, J. A.; White, M. G.; Liu, P. *Phys. Chem. Chem. Phys.* **2010**, *12*, 9909−9917. (b) Liao, F.; Huang, Y.; Ge, J.; Zheng, W.; Tedsree, K.; Collier, P.; Hong, X.; Tsang, S. C. *Angew. Chem., Int. Ed.* **2011**, *50*, 2162−2165.
(20) Zheng, J.; Lin, H.; Wang, Y.-n.; Zheng, X.; Duan, X.; Yuan, Y. *J. Catal.* **2013**, *297*, 110−118.
(21) Clarke, M. L.; Roff, G. J. *Handb. Homogeneous Hydrogenation* **2007**, 413−454.